This is a repository copy of *Prediction of alkaline earth elements in bone remains by near infrared spectroscopy*.

White Rose Research Online URL for this paper:
https://eprints.whiterose.ac.uk/110415/

Version: Accepted Version

Article:

1   **PREDICTION OF ALKALINE EARTH ELEMENTS IN BONE REMAINS BY NEAR INFRARED**

2   **SPECTROSCOPY**

3   Mari Merce Cascant, Sonia Rubio, Gianni Gallello*, Agustín Pastor, Salvador Garrigues and

4   Miguel de la Guardia.

5   Department of Analytical Chemistry, University of Valencia,

6   50 Dr. Moliner Street, research building

7   46100 Burjassot, Valencia, Spain.

8   * Corresponding author

9

10   **Abstract**

11   An innovative methodological approach has been developed for the prediction of the

12   mineral element composition of bone remains. It is based on the use of Fourier Transform

13   Near Infrared (FT-NIR) diffuse reflectance measurements. The method permits a fast,

14   cheap and green analytical way, to understand post-mortem degradation of bones caused

15   by the environment conditions on different skeletal parts and to select the best preserved

16   bone samples. Samples, from the Late Roman Necropolis of Virgen de la Misericordia

17   street and En Gil street located in Valencia (Spain), were employed to test the proposed

18   approach being determined calcium, magnesium and strontium in bone remains and

19   sediments. Coefficients of determination obtained between predicted values and

20   reference ones for Ca, Mg and Sr were 90.4, 97.3 and 97.4, with residual predictive

21   deviation of 3.2, 5.3 and 2.3, respectively, and relative root mean square error of

22   prediction between 10 and 37%. Results obtained evidenced that NIR spectra combined

23   with statistical analysis can help to predict bone mineral profiles suitable to evaluate bone

24   diagenesis.

1. Introduction

Bone is composed of 50 to 70% mineral, 20 to 40% organic matrix, mainly collagen, 5 to 10% water, and less than 3% lipids. The mineral content of bone is mostly hydroxylapatite $[Ca_{10}(PO_4)_6(OH)_2]$, with small amounts of carbonate, magnesium, and acid phosphate, with missing hydroxyl groups that are normally present [1]. Under physiologic conditions, hydroxylapatite is the only stable mineral in bones and is composed of 38% of calcium and 18% of phosphorous, with trace of sodium (0,6%), magnesium and small amount of other elements [2]. The number of ionic substitutions possible in biological apatite is smaller than in geologic apatites due to the limited number of available elements in the body. Among the substituting ions that are known and/or reported in bone and tooth mineral are F^-, Cl^-, Na+ , K^+ , Fe^{2+}, Zn^{2+}, Sr^{2+}, Mg^{2+}, citrate, and carbonate [3].

Minerals are ingested from food or involuntary absorbed from the environment. Chemical composition of bones mineral is commonly employed to investigate pathologies, nutrition, injuries and other bioarchaeological and forensic issues.

The mineral composition of bones can be post-mortem modified by post-depositional processes, called as well diagenesis, and since many decades researchers have been intensively studied these natural mechanisms. Some authors have evaluated post-mortem soil contamination in bones [4-9]. Other authors have studied diagenesis and degradation effects on bone matrix [10-13].

48 Calcium, oxygen and hydrogen are major constituents of mineral bones as hydroxylapatite

49 [14]. Strontium is a non-essential trace element that competes to replace calcium[15]and

50 has been linked to food consumption habits [16]. The soil composition and environmental

51 conditions play a crucial role in diagenesis, affecting the element concentration of the

52 buried bones.

53 The general aims of this study has been to develop a low cost, clean and fast strategy to

54 understand how post-mortem degradation in bones caused by the environment could

55 affect different skeletal parts and define an approach to select the best preserved bone

56 samples. Therefore, a method for the determination of mineral elements in bone remains

57 has been developed employing Fourier Transform Near Infrared (FT-NIR) spectroscopy by

58 using chemometric tools as principal component analysis (PCA) and Partial Least Square

59 (PLS). Inductively-Coupled Plasma Optical Emission Spectroscopy (ICP-OES) results have

60 been used as reference data to create prediction models.

61 ICP-OES has been commonly used as an accurate procedure to determine mineral

62 elements in soils and bones [17-21]. ICP-OES technique is very useful for multi-element

63 analysis. However it requires a previous sample digestion and dissolution, involving the

64 use of strong acids and providing non-degradable wastes. A green alternative to the

65 aforementioned technique could be infrared (IR) spectroscopy which provides fast

66 spectral acquisition, a cheap acquisition and maintenance cost and a sustainable method,

67 since it does not use reagents and can be employed directly on solid samples.

68 Combination of IR spectroscopy with chemometric data analysis could offer a significant

69   tool for the determination of major components of bones and sediments including

70   mineral elements.

71   Fourier Transform infrared (FT-IR) spectroscopy of bones has been used for various

72   applications as collagen determination, bone crystal size, some carbonates and crystalline

73   structure [22-25], and geochemical taphonomy [26] and as screening tool for diagenetic

74   alteration [27, 28]. On the other hand, only few studies have employed NIR for soils [29]

75   and bones analysis [30] in archaeological contexts.

76

77   In the present study, two hundred seventy one samples obtained from at least 78

78   individuals, have been analyzed. Samples belong to adult and young individuals and are

79   from the Late Roman Necropolis of Virgen de la Misericordia Street [19] and en Gil Street

80   [31], both located in the city of Valencia (Spain). The Late Roman burial rite consisted in

81   inhumation. At this sites, the tombs belong to the period from the I century A.D. until the

82   beginning of the V century A.D.

83   Bone samples were collected from femur, tibia, humerus, radius and parietal bones, which

84   were classified as cortical bones, and ribs as spongy bones. Furthermore, bone samples

85   from the outer bone layer and soil samples were analyzed. Outer bone layer samples were

86   obtained from the external bone surface directly in contact with the sediments. Principal

87   Component Analysis (PCA) was applied to identify bone samples with a well preserved

88   elemental composition. Therefore for the first time Partial Least Square (PLS) regression

89   models were built to predict the concentration of calcium, magnesium and strontium in

90   skeletal remains by NIR spectra of the mineralized and homogenized solid samples.

91

2. Materials and methods

2.1. Sample collection

94

Bone samples were collected from 78 different individuals, sampling around 5 cm of each

bone and the weight of the collected sample ranged between 15 and 20 grams depending

on the type of bone. Bones as femur, tibia, humerus, radius and parietals,   mainly

composed by a cortical matrix were classified as "cortical", and ribs mainly composed by a

spongy matrix were grouped as "spongy".   The first 2 mm of bone directly in contact

with the sediments was called external part of bones and was obtained employing a

bistoury to scrape. All bones were sampled avoiding the osteometric points, and the

sampling was carried out using a cutting toll and a micro spoon spatula.

To provide reproducible and comparable results compatible with the sensitivity of the

analytical methods employed and so appropriately relate NIR obtained data with the

reference method data all samples were previously mineralized in a muffle furnace,

(temperature programme employed: I. 30min at 150 ^{o}C; II. 1° /min up to 450 ^{o}C; III. 24h at

450 ^{o}C; IV. 30 ^{o}C), and pulverized and homogenized with an agate mortar

108

A total of 243 samples from Virgen de la Misericordia were analysed. Bone samples were

divided in three groups: i) internal part of bones, composed by the internal part of cortical

and spongy ones (95 samples), ii) external part of bones, composed by the first external

layer of cortical bones and spongy ones (94 samples) and, iii) sediments that were directly

113 in contact with the bones (54 samples). Additionally following the mentioned

114 classification, 28 samples from En Gil internal part of bones (8 samples), external part of

115 bones (10 samples) and sediments (10 samples) were also analyzed.

116

117 **_2.2. Apparatus and methods_**

118 For diffuse reflectance near infrared spectra acquisition, a Fourier transform near infrared

119 spectrometer, model Multipurpose Analyzer (MPA) from Bruker (Bremen, Germany),

120 equipped with an integrating sphere was employed. This instrument is equipped with a

121 NIR source, a quartz beamsplitter and PbS detector. For instrumental and measurement

122 control as well as for data acquisition, Opus 6.5 software from Bruker was used.

123

124 References values about the mineral composition of samples were determined by using an

125 Optima 5300 DV ICP-OES Perkin Elmer (Norwalk, CT, USA) equipped with an autosampler

126 AS 93-plus and a cross flow nebuliser. Samples were previously calcinated inside a muffle

127 furnace Biometa Lenton ECF 12145A (Lanera, España) and acid digested using a heating

128 plate Ika C-Mag HS7.

129

130 **_2.3. Reference method_**

131 The digestion method was developed modifying the process described by Gallello et al.

132 2013 and 2014 [19] and consisted in addition to 0.5 g of mineralized sample of 1:1 HCl and

133 HNO_3 (using 37 % HCl and 69 % HNO_3 high purity stock) and digested in a water bath at

134 100° C. This concentrated solution (A), was diluted 1:250 obtaining solution (B), to

135 measure Mg and Sr. Solution (C) was obtained to analyze Ca by diluting 1:2000 solution

136 (A). Concentrations of HCl and HNO_3 have been maintained constant in all solutions. A

137 multi-element stock solution containing Ca, Mg and Sr at a concentration of 100 µg ml^{-1}

138 was employed for the preparation of the calibration standards in 50 ml volumetric flasks.

139 To avoid the obstruction of the nebulizer system samples were filtered employing filter

140 paper (WhatmanTM N.1 of 70mm). Concentrations ranging between 0 and 20 µg ml^{-1}

141 were used for Ca, Mg and Sr. Standards were obtained from Sharlab S.L. (Barcelona,

142 Spain). The standard error of readings during the analysis ranged from 0 % to 2 % for the

143 major elements considered. Bone ash NIST 1400 and soil GBW07408 were used as

144 standard reference materials for evaluating the accuracy of the analytical method and Re

145 was used as internal standard. Mineral element content of studied samples, determined

146 by reference method, varied between 72 and 421 mg g^{-1} for calcium, 998 and 10964 µg g^{-1}

147 for magnesium and, 102 and 2100 µg g^{-1} for strontium.

148

149 ***2.4. NIR procedure***

150 Pulverized mineralized samples were placed in clear glass vials of 11 mm internal diameter

151 and 25 mm height to directly obtain their NIR spectra by diffuse reflectance in Kubelka–

152 Munk units. Spectra were collected between 14000 and 4000 cm^{-1} by averaging 50 scans

153 and using an optical resolution of 4 cm^{-1}. A background spectrum was acquired before

154 each series, from the closed integrating sphere using the same instrumental conditions

155 than those employed for samples measurement. Three measurements of each sample

156 were obtained by rotating the sample vial position between replicates in order to ensure a

157   good reliability. The average of the triplicate spectra of each sample was employed for

158   data exploration and to build the chemometric models.

159

160   ***2.5. Chemometric data treatment***

161   Data treatment was carried out using in-house written functions employing Matlab

162   8.3.0.532 (R2014a) from Mathworks (Natick, MA, USA) being employed for Principal

163   Analysis Components (PCA) and Partial least squares (PLS) regression model, the PLS

164   Toolbox 7.5.2 from Eigenvector Research Inc. (Wenatchee, WA, USA).

165   PCA applied to IR spectra was used as data exploration; based on the distance between

166   samples the evaluation of their similarity. PLS models were applied to spectral data to

167   develop prediction models for Ca, Mg and Sr. These calibration models were developed

168   based on the statistically inspired modification of the PLS method (SIMPLS) algorithm

169   [32]. To select the most appropriate sample calibration set, Kennard–Stone (KS)

170   algorithm [33] was used, thus selecting a representative subset to ensure training

171   samples spread evenly throughout the sample space. For building the best PLS models,

172   different spectral regions and spectra pre-treatments were tested as multiplicative

173   scatter correction (MSC), standard normal variation (SNV), a Savitzky-Golay first (FD) and

174   second derivative (SD), and mean center (MC) also combination of them. The

175   performance of PLS-NIR models was evaluated according to the root mean square error

176   of cross validation and prediction (RMSECV and RMSEP) values, the coefficient of

177   determination for prediction (R^2pred), relative root mean square error of prediction

178   (RRMSEP) and residual predictive deviation (RPD), calculated this last parameter as the

179   ratio between standard deviation (SD) of the prediction set and the RMSEP values [34].

180   Generally, RPD value greater than 3.0 is considered adequate for analytical purposes with

181   excellent prediction accuracy, between 2.5 and 3.0 implies that the model has a good

182   precision and between 2.0 and 2.5 indicates that the model has an approximate

183   precision. A value for the RPD between 1.5 and 2.0 reveals a possibility to distinguish

184   between high and low values and a RPD 1.5 indicates that the calibration is not usable

185   [35]. The optimum number of latent variables (LV's) was determined by cross-validation

186   using leave one out sample in order to obtain the minimum value of RMSECV.

187

188   **3. Results and discussion**

189   *3.1. FT-NIR spectra*

190   Figure 1 shows, in Kubelka Munk units, the averaged NIR spectra of a) internal part, b)

191   external part of bones and c) sediment samples, considered in this study without any data

192   pre-treatment, in the region between 9000 and 4000 cm^{-1}. These sample spectra present

193   differences in the intensity and position of certain bands, but all show absorption bands

194   around 7200 and 5220 cm^{-1} related to combination vibrations of H–O–H bend and O–H

195   stretch of water. The main difference which presents internal bones is the weak vibration

196   which appear near 4655 cm^{-1} (without a clear assignment) and the absorption near 6977

197   cm^{-1} assigned to the first overtone of the stretching vibrations of OH group in

198   hydroxyapatite [36], that is higher than in external part of bones. In the case of the

199   sediment samples, the aforementioned band is absent. Additionally, at 5278 cm^{-1}, internal

200   part of bone and external part of bone in minor intensity, present an absorption band

201   related to apatite [30]. On the other hand, in sediment samples it is present a band at

202   7070 cm^{-1} related to the first overtone of the O–H stretch vibration in metal–O–H [37].

203   Moreover, vibrations bands near of 4530 cm^{-1} are due to clay minerals, like smectite and

204   illite, and the band at 4265 cm^{-1} is associated with the contribution of calcite [37], which

205   decreases in intensity in external bone. In the case of internal part of bone samples, the

206   band located at 4265 cm^{-1} not appears and the band at 4530 cm^{-1} is less intense than in

207   external part of bones. So that, in external part of bones appear typical bands of sediment

208   samples related with metal-OH (7070 cm^{-1}), calcite (4265 cm^{-1}) and clay minerals (4530

209   cm^{-1}), and lower bands of hydroxyapatite (6977 cm^{-1}) and apatite (5278 cm^{-1}).

210   Degradation of hydroxyapatite in external part of bones is a great indicator of diagenetic

211   process. Sediments around bones are crucial role to conservation of them, and sediments

212   analysis should be carried out in order to assess their contribution to the modification of

213   the bone chemical composition.

214

215

216   ***3.2. Data Exploration by PCA***

217   Before building the calibration models, PCA was used for exploratory data analysis to

218   study the spectral differences between considered samples. Figure 2 presents the scores

219   plot for first and the second principal components obtained from PCA for Misericordia and

220   En Gil Necropolis, after a) FD and MC and b) MSC, FD and MC pre-treatment, being

221   selected the region from 9014 to 4000 cm^{-1}. In Figure 2a, the two first principal

222   components after spectra pretreatment by using FD and MC represent 86.07% of the

223   explained variance, being 76.93 and 9.14% for PC1 and PC2, respectively. In the scores

224   plot, there is not a clear-cut grouping of samples, but it can be appreciated that sediment

225   samples spectra are clearly different from those of internal part of bone samples and that,

226   external part of bone samples are located between sediment and internal part of bone

227   ones in the direction of PC1. In Figure 2b, it can be seen that the scores plot for first and

228   the second principal components after MSC, FD and MC pretreatment, represent 85.72%

229   of the explained variance (PC1 corresponds to 80.49% and PC2 corresponds to 5.23% of

230   the variance). It can be seen that internal part of bone samples are located towards the

231   right of the PC1 and sediment samples are dispersed in the left. External part of bone

232   samples are situated between these two groups in the direction of PC1. Moreover, PCA

233   indicates that samples derived from En Gil are similar to Misericordia samples, and

234   because of that samples from Misericordia can be used as calibration set to predict

235   alkaline earth elements in En Gil samples.

236   The aforementioned PCAs were built using differentiated internal and external parts of

237   bones in both, spongy and cortical remains. Figure 2c presents the scores plot after FD and

238   MC and Figure2d after MSC, FD and MC pretreatment. No differences were detected

239   between internal parts of cortical and spongy bones. However if we look at the external

240   part of bones, spongy group is located near to sediment samples, and external part of

241   cortical bones are located close to internal part of bones because spongy tissues are more

242   susceptible to diagenesis than cortical [38] due to the fragility and porosity of their

243   structure. Wavenumbers responsible for the distinction of the samples in PCA can be

244   identified in the corresponding loading plots (Figure 2e and 2f) with a clear identification

245   of bands around 7000 cm^{-1} and between 5500 and 4000 cm^{-1}.

246

247   So, it can be concluded that PCA analysis using NIR spectra data provides a fast and green

248   tool to identify changes caused by the environment in bone samples. These results

249   indicate that external part of bones suffer an increased degradation produced by

250   diagenetic factors than internal part of bones, especially in the case of spongy bones

251   external part due to their high porosity. Consequently, conclusions about identification of

252   biogenetic signals using major element ratios could change depending of the bone class

253   evaluated. To avoid mistakes, the use of PCA analysis, as exploratory method, permits a

254   prior selection of samples, not affected by diagenetic processes, to be used in different

255   bioarchaeological and forensic studies involved in bone analyses. Additionally, PCA is a

256   good indicator to test if the calibration set contains the validation samples in order to be

257   used in PLS models without errors due to extrapolation of data.

258

259   ***3.3. PLS-NIR models***

260   To build PLS models, Misericordia samples were divided into a calibration and a validation

261   subset with 183 and 60 objects, respectively, using K-S algorithm for the training set

262   selection, composed by 62 external part of bones, 70 internal part of bones and 51

263   sediment samples.

264   The main characteristics of calibration and validation sets selected for the three elements

265   determination by PLS-NIR are indicated in Table 1. Several regions and different pre-

266   processing strategies were assayed to build the best models and to evaluate their

267   prediction capability. For all elements, regions selected were those between 9014 and

268   4000 cm^{-1}. To build PLS-NIR models using the selected spectral range, 3, 4 and 4 LVs were

269   employed for Ca, Mg and Sr, respectively, in order to minimize the RMSECV, explaining

270   89.1 %, 90.8 % and 88.5 % of the total variance of the X data block and 92.4%, 95.0% and

271   90.4% of the Y data block, respectively. For Ca and Mg, FD with a window of 11 points and

272   a second order polynomial, and MC treatment were adopted as signal pre-processing. For

273   strontium, MSC, FD and MC were chosen. Additionally, concentration data were mean

274   centered as well in all cases. Outliers can be identified by Q residual versus the Hotelling

275   T^2 values, being removed 2 samples from the calibration set of Ca, Mg and Sr and 2

276   samples from the validation set of Ca and Sr and only one sample of Mg, prior to do the

277   calculations and validation of the final PLS models for those elements. Figure 3a shows the

278   regression between PLS-NIR predicted values for Ca, Mg and Sr and those obtained by the

279   reference ICP-OES method. It can be seen that calibration and validation sample points

280   were closely distributed near the optimum regression line between predicted and

281   measured values for the three elements, obtaining high coefficients of determination for

282   calibration (R^{2}cal), cross validation (R^{2}CV) and prediction (R^{2}pred) in all elements. The

283   prediction capability of PLS-NIR models were good for all elements, obtaining RRMSEP

284   values of 10%, 15% and 19% for calcium, magnesium and strontium, respectively. The

285   most important calibration and validation parameters of the developed PLS-NIR models

286   are summarized in Table 2.

287

288   It can be seen that samples of internal part of bones contain higher calcium (368 ± 24 mg

289   g^{-1}) and strontium (1306 ± 235 µg g^{-1}) levels and lower magnesium content (1393 ± 175 µg

290   g^{-1}) than external parts (with 261 ± 47 mg g^{-1} of Ca, 844 ± 203 µg g^{-1} of Sr and 5599 ± 1684

291   µg g^{-1} of Mg) and sediment samples (with 133 ± 17 mg g^{-1} of Ca, 239 ± 60 µg g^{-1} of Sr and

292   8165 ± 858 µg g^{-1} of Mg). As aforementioned, in physiologic conditions, hydroxylapatite is

293   composed of 38 % Ca, with traces of Mg and small amounts of other elements like Sr,

294   indicating that internal part of bones are intact looking at Ca values that are around

295   the38%. Mg enrichment in external part of bones indicates that this element is probably

296   incorporated into the bones from sediments during diagenesis process.

297   External part of bones, especially in the case of spongy bone remains are more sensitive to

298   diagenetic processes caused by the environment indicating that degradation not affects in

299   the same extent different skeletal parts. Due to the fact that spongy bones have higher

300   porosity and thinner cortex than cortical bones, the first type is less resistant to diagenetic

301   factors suffering chemical changes.

302

303   Results obtained by PLS-NIR models indicated that NIR spectroscopy has a good potential

304   to predict alkaline earth elements content in bone remains. As mentioned this method has

305   many advantages over the conventional employed analytical techniques because it is

306   quick, inexpensive, non-destructive for pulverized samples and does not require the use of

307   chemical reagents nor solvents.

308

309   *3.4. PLS-NIR prediction capability*

310 To evaluate the PLS-NIR prediction capability of models built to predict Ca, Mg and Sr

311 concentrations in bones and sediments, an independent validation set, not employed

312 during the calibration step, was used. For this propose external part, internal part of

313 bones and sediment samples of En Gil Necropolis were used as external set. The mean,

314 concentration range and standard deviation for the concentration of analysed elements

315 employed for prediction set are summarized in Table 1. Predicted values of the analytes

316 versus those obtained by the reference methods are shown in Figure 3b and the most

317 important calibration and prediction parameters of the developed NIR-PLS models are

318 summarized in Table 2. Acceptable RRMSEP values were obtained for calcium and

319 magnesium with 15% and 11%, respectively, and for strontium a value of 37% was

320 obtained, with correlation coefficients of 90.4, 97.4 and 97.4, and RPD values of 3.2, 5.33

321 and 2.3, respectively. These results demonstrate a good predictive capability of the PLS-

322 NIR models developed to evaluate alkaline earth elements in bones and sediment

323 samples.

324

325 Furthermore it must be indicated the PLS models were made from bone samples of

326 different origin, and date of those of the training set, confirming the feasibility of our

327 innovative methodological proposal for the evaluation of alkaline earth elements in

328 archaeological remains.

329

330 The obtained results indicate a good predictive capability for Mg in samples that not

331 belong to the same population while Ca were predicted with relative errors of 15% and Sr

332 37%, respectively, being thus limited as a screening tool. Especially for Sr the high relative

333 error of 37% is probably due to the lower levels of this element found in some samples

334 not compatible with the sensitivity of NIR.

335

336

337 **4. Conclusions**

338 Fourier Transform Near Infrared (FT-NIR) provides a fast, cheap and green analytical

339 method for the prediction of the content of calcium, magnesium and strontium in buried

340 bone and sediment samples, and it could be very useful to understand post-mortem

341 changes of bones caused by the environment which can affects different skeletal parts

342 and for selecting bone samples with well preserved biogenetic signals. PCA has shown that

343 the alkaline earth element profile of bone and soil samples, as expected, is clearly

344 different. Furthermore the external surface of spongy bones is more similar to the soils

345 than to the surface of cortical bones. This confirm that the outer bone layer of spongy

346 bones is more altered than the cortical surface and the presence of Ca, Mg and Sr is

347 similar to that of soil samples of the studied sites. Therefore it can be concluded that

348 environmental factors have a main impact on spongy tissues, which are more susceptible

349 to diagenetic processes, than on the cortical bones. It is indicated in the NIR spectra by the

350 loss of apatite band (the main bone compound) and the presence of clay bands especially

351 on spongy bone surface.

352 A milestone in the study of bone remains is settled in this work by the development of

353 PLS-NIR models, indicating that FT-NIR spectroscopy can be employed to predict Ca, Mg

354 and Sr contents in bones remains and soils samples. Ca and Sr contents were found to be

355 higher in the internal part of bone samples, opposite to Mg contents that were higher in

356 the external bone surface and soils, and lower in internal part of bones. Our developed

357 methodological approach combines NIR spectroscopy and statistical analysis and this

358 allowed us to predict bone alkaline earth mineral composition opening a new perspective

359 for the identification of better preserved samples in bioarchaeological studies and forensic

360 science investigations.

361 Regarding the limitations of the study it must be noticed that it was based only on the

362 mineral part of skeletal remains which were treated thermally and pulverized before

363 measurements thus losing information from the organic part of bones and soils.

364 Additionally, the lack of sensitivity of NIR spectroscopy seriously affected the capability of

365 these measurements to be employed for trace element determination and just important

366 elements present as major components of bones, like Ca, Mg and Sr could be determined.

367

373 The authors would like to thanks all the students of Chemistry and Archaeology which

374 have contributed to the realization of this study.

375

376

References

378 [1] B. Clarke, Normal bone anatomy and physiology, Clin. J. Am. Soc. Nephrol. 3 (2008) Suppl 3,
379   S131–139.

380 [2] J. Burton, Bone chemistry and trace element analysis. in M.A. Katzenberg, S.R. Saunders
381   (Eds.) Biological anthropology of the human skeleton. 2nd ed. John Wiley & Sons, Inc.,
382   Hoboken, NJ (2008) 443–460.

383 [3] B. Wopenka and J. D. Pasteris, A mineralogical perspective on the apatite in bone, Mater. Sci.
384   Eng. C, 25 (2005) 131–143.

385 [4] R. E. M. Hedges and A. R. Millard, Bones and Groundwater: Towards the Modelling of
386   Diagenetic Processes, J. Archaeol. Sci., 22 (1995) 155–164.

387 [5] R. E. M. Hedges, Bone diagenesis: an overview of processes, Archaeometry, 44 (2002) 319–
388   328.

389 [6] W. Querido, A. L. Rossi, and M. Farina, The effects of strontium on bone mineral: A review on
390   current knowledge and microanalytical approaches, Micron, 80 (2016), 122–134.

391 [7] J. B. Lambert, L. Xue, and J. E. Buikstra, Inorganic analysis of excavated human bone after
392   surface removal, J. Archaeol. Sci., 18 (1991) 363–383.

393 [8] F. Donald Pate and J. T. Hutton, The Use of Soil Chemistry Data to Address Post-mortem
394   Diagenesis in Bone Mineral, J. Archaeol. Sci., 15 (1988) 729–39.

395 [9] J. Zapata, C. Pérez-Sirvent, M.Martínez-Sánchez, and P. Tovar, Diagenesis, not biogenesis:
396   Two late Roman skeletal examples,Sci. Total Environ., 369 (2006) 357–368.

397 [10] I. Reiche, L. Favre-Quattropani, Calligaro, T. J. S., H. Bocherens, L. Charlet, M. Menu, Trace
398   element composition of Archaeological Bones and postmortem alteration in the burial
399   environment. Nuclear Instruments and Methods. Physics Research B 150 (1999) 656-662.

400 [11] I. Reiche, L. Favre-Quattropani, C. Vignaud, H. Bocherens, L. Charlet, M. Menu, A multi-
401   analytical study of bone diagenesis: the Neolithic site of Bercy (Paris, France). Meas. Sci.
402   Technol. 14 (2003)1608-1619.

403 [12] T.H. Schmidt-Schultz, M. Schultz, Intact protein molecules in archaeological bones – Bone
404   matrix as a treasure chest of ancient diseases and living conditions. American Journal of
405   Physical Anthropology. Annual Meeting Issue l999, Wiley-Liss, p. 230.

406 [13] T. A. Surovell and M. C. Stiner, Standardizing Infra-red Measures of Bone Mineral
407   Crystallinity: an Experimental Approach, J. Archaeol. Sci., 28(2001) 633–642.

408 [14] F. Ignac, G. Gopinath, and V. der W. Hans, Radionuclide and Hybrid Bone Imaging. Springer
409   Heidelberg New York Dordrecht London, 2012.

410   [15] M. L. Carvalho and A. F. Marques, Diagenesis evaluation in Middle Ages human bones using
411   EDXRF, X-Ray Spectrom., 37 (2008) 32–36.

412   [16] D. Guimarães, A. A. Dias, M. Carvalho, M. L. Carvalho, J. P. Santos, F. R. Henriques, F. Curate,
413   and S. Pessanha, Quantitative determinations and imaging in different structures of buried
414   human bones from the XVIII-XIXth centuries by energy dispersive X-ray fluorescence –
415   Postmortem evaluation, Talanta, 155 (2016) 107–115.

416   [17] G. Gallello, J. Kuligowski, A. Pastor, A. Diez, and J. Bernabeu, Biological mineral content in
417   Iberian skeletal cremains for control of diagenetic factors employing multivariate statistics, J.
418   Archaeol. Sci., 40(2013) 2477–2484.

419   [18] A.-F. Maurer, M. Gerard, A. Person, I. Barrientos, C. R. del, V. Darras, C. Durlet, V. Zeitoun, M.
420   Renard, and B. Faugère, Intra-skeletal variability in trace elemental content of Precolumbian
421   Chupicuaro human bones: The record of post-mortem alteration and a tool for palaeodietary
422   reconstruction, J. Archaeol. Sci., 38 (2011) 1784–1797.

423   [19] G. Gallello, J. Kuligowski, A. Pastor, A. Diez, and J. Bernabeu, Chemical element levels as a
424   methodological tool in forensic science, J Forensic Res, 6 (2014) 1000264.

425   [20] A.-F. Maurer, A. Person, T. Tütken, S. Amblard-Pison, and L. Ségalen, Bone diagenesis in arid
426   environments: An intra-skeletal approach, Palaeogeogr. Palaeoclimatol. Palaeoecol., 416
427   (2014) 17–29.

428   [21] S. Dal, L. Maritan, D. Usai, I. Angelini, and G. Artioli, Bone diagenesis at the micro-scale: Bone
429   alteration patterns during multiple burial phases at Al Khiday (Khartoum, Sudan) between
430   the Early Holocene and the II century AD, Palaeogeogr. Palaeoclimatol. Palaeoecol.,
431   416(2014) 30–42.

432   [22] S. W. Keenan, A. S. Engel, A. Roy, and G. Lisa Bovenkamp-Langlois, Evaluating the
433   consequences of diagenesis and fossilization on bioapatite lattice structure and composition,
434   Chem. Geol., 413 (2015) 18–27.

435   [23] C. N. Trueman, K. Privat, and J. Field, Why do crystallinity values fail to predict the extent of
436   diagenetic alteration of bone mineral?, Palaeogeogr. Palaeoclimatol. Palaeoecol., 266
437   (2008)160–167.

438   [24] T. J. U. Thompson, M. Islam, K. Piduru, and A. Marcel, An investigation into the internal and
439   external variables acting on crystallinity index using Fourier Transform Infrared Spectroscopy
440   on unaltered and burned bone, Palaeogeogr. Palaeoclimatol. Palaeoecol., 299(2011) 168–
441   174.

442   [25] T. J. U. Thompson, M. Islam, and M. Bonniere, A new statistical approach for determining the
443   crystallinity of heat-altered bone mineral from FTIR spectra, J. Archaeol. Sci., 40 (2013) 416–
444   422.

445   [26] G. Iliopoulos, N. Galanidou, S. A. Pergantis, V. Vamvakaki, and N. Chaniotakis, Identifying the
446   geochemical taphonomy of the osteological material from Katsambas rockshelter, J.
447   Archaeol. Sci., 37 (2010) 116–123.

448　　[27] L. E. Wright and H. P. Schwarcz, Infrared and Isotopic Evidence for Diagenesis of Bone Apatite
449　　　　　at Dos Pilas, Guatemala: Palaeodietary Implications, J. Archaeol. Sci., 23 (1996) 933–944.

450　　[28] D. Alfano, A. R. Albunia, O. Motta, and A. Proto, Detection of diagenetic alterations by
451　　　　　Spectroscopic Analysis on Archaeological Bones from the Necropolis of Poseidonia
452　　　　　(Paestum): A case study, J. Cult. Herit., 10 (2009) 509–513.

453　　[29] J. Linderholm and P. Geladi, Classification of archaeological soil and sediment samples using
454　　　　　near infrared techniques, NIR News, 23 (2012) 6.

455　　[30] D. Thomas, C. McGoverin, A. Chinsamy, and M. Manley, Near infrared analysis of fossil bone
456　　　　　from the Western Cape of South Africa, J. Infrared Spectrosc., 19(2011) 151.

457　　[31] G. Gallello, S. Silvia, J. Kuligowski, B. Fulvio, M. Francesco, and P. Agustín, Variación química
458　　　　　intraesquelética relacionada con la diagénesis en los restos óseos de c/ en Gil (Valencia),
459　　　　　SAGVNTVM, 47 (2015) 175–186.

460　　[32] S. de Jong, SIMPLS: An alternative approach to partial least squares regression, Chemom.
461　　　　　Intell. Lab. Syst., 3 (1993) 251–263.

462　　[33] R. W. Kennard and L. A. Stone, Computer Aided Design of Experiments, Technometrics, 11
463　　　　　(1969) 137–148.

464　　[34] P.C. Williams, D. Sobering, How do we do it: A brief summary of the methods we use in
465　　　　　developing near infrared calibrations, A.M.C. Daves, P.C. Williams (Eds.), Near infrared
466　　　　　spectroscopy: The future waves, NIR Publications, Chichester, UK (1995) 185–188.

467　　[35] W. Saeys, A. M. Mouazen, and H. Ramon, Potential for Onsite and Online Analysis of Pig
468　　　　　Manure using Visible and Near Infrared Reflectance Spectroscopy, Biosyst. Eng., 91(2005)
469　　　　　393–402.

470　　[36] Y. Ning, J. Li, W. Cai, and X. Shao, Simultaneous determination of heavy metal ions in water
471　　　　　using near-infrared spectroscopy with preconcentration by nano-hydroxyapatite,
472　　　　　Spectrochim. Acta. A. Mol. Biomol. Spectrosc., 96 (2012) 289–294.

473　　[37] V. Aranda, A. Domínguez-Vidal, F. Comino, J. Calero, and M. J. Ayora-Cañada, Agro-
474　　　　　environmental characterization of semi-arid Mediterranean soils using NIR reflection and
475　　　　　mid-IR-attenuated total reflection spectroscopies, Vib. Spectrosc., 74 (2014) 88–97.

476　　[38] J.B. Lambert, S.M. Vlasak, A.C. Thometz, J.E. Buikstra, A comparative study of the chemical
477　　　　　analysis of ribs and femurs in Woodland population, American Journal of Physical
478　　　　　Anthropology 59 (1982) 289-294.
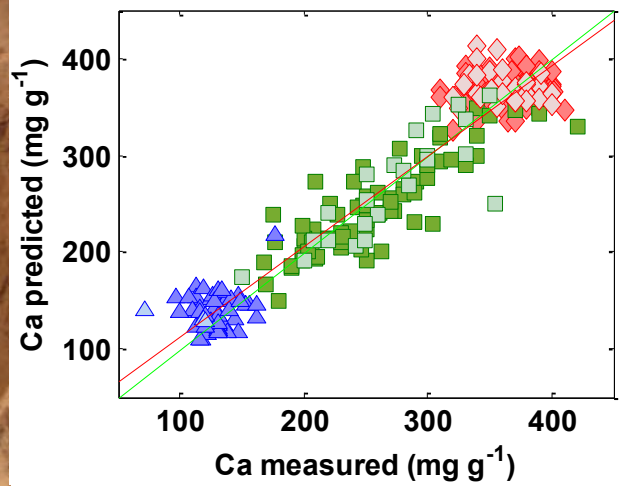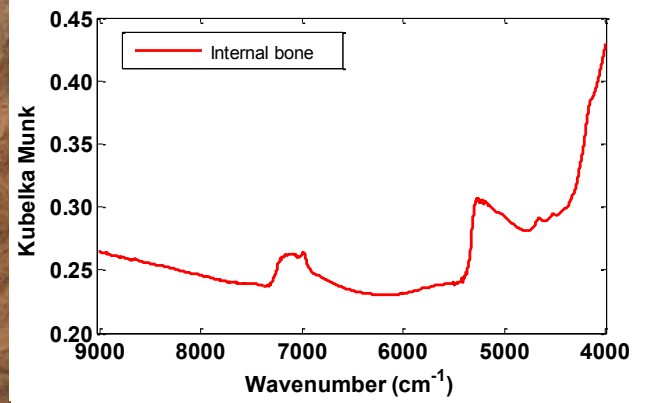
479

Graphical Abstract

Table 1. Concentration ranges of determined mineral elements in calibration, validation and prediction data sets

Analyte	Set	Samples	Range	Mean value	SD
Calcium (mg g^{-1})		181	96 - 421	260	100
Magnesium (µg g^{-1})	Calibration	181	1050 - 10500	4967	3091
Strontium (µg g^{-1})		181	153 - 2100	823	486
Calcium (mg g^{-1})		58	72 - 400	312	76
Magnesium (µg g^{-1})	Validation	59	1070 - 8500	3226	2545
Strontium (µg g^{-1})		58	124 - 2010	1058	405
Calcium (mg g^{-1})		26	112 - 421	233	114
Magnesium (µg g^{-1})	Prediction	26	998 - 10964	6723	3864
Strontium (µg g^{-1})		26	102 - 1350	518	442

SD: Standard deviation

Table 2. Description of the best PLS-NIR models employed for the determination of Ca, Mg and Sr and their main figures of merit.

Element	Pre-process	LV	Misericordia samples								en Gil samples						
			RMSEC	R^2 Cal	RMSECV	R^2 CV	RMSEP	R^2 Pred	RRMSEP (%)	RPD	RMSEP	R^2 Pred	Slope	Intercept	Bias	RRMSEP (%)	RPD
Calcium (mg g^{-1})	FD, MC	3	27.5	92.4	29.0	91.6	31.7	83.4	10.2	2.4	35.6	90.4	0.8299	41.4	1.7	15.3	3.2
Magnesium (µg g^{-1})	FD, MC	4	686.3	95.0	750.2	94.1	496.6	96.3	15.4	5.1	723.7	97.3	0.9504	246.2	-81.3	10.8	5.3
Strontium (µg g^{-1})	MSC, FD, MC	4	150.1	90.4	169.8	87.7	198.9	76.2	18.8	2.0	198.9	97.4	0.9041	78.9	155.0	37.3	2.3

LV: number of latent variables

RMSEC: Root mean square error of calibration; RMSECV: Root mean square error of cross validation; RMSEP: Root mean square error of prediction; RRMSEP: Relative root mean square error of prediction; R^2 Cal: coefficient of determination of calibration; R^2 CV: coefficient of determination of cross validation; R^2 Pred: coefficient of determination of prediction.
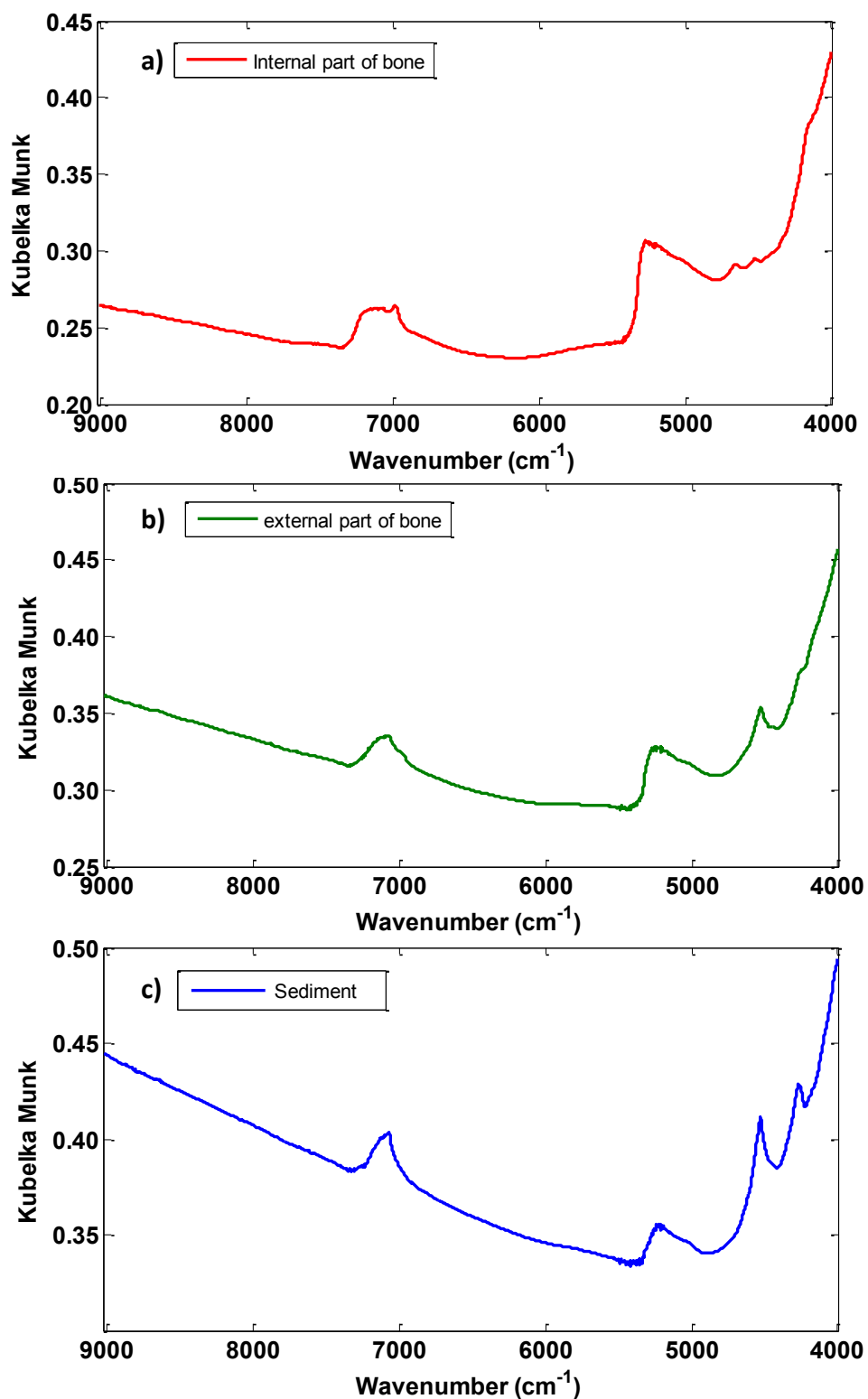
Figure 1. Averaged NIR spectra of mineralized bone and sediment samples comparing **a)** internal part, **b)** external part, and **c)** sediment samples. Note: Spectra were in Kubelka Munk units in the region between 9000 and 4000 cm^{-1}.
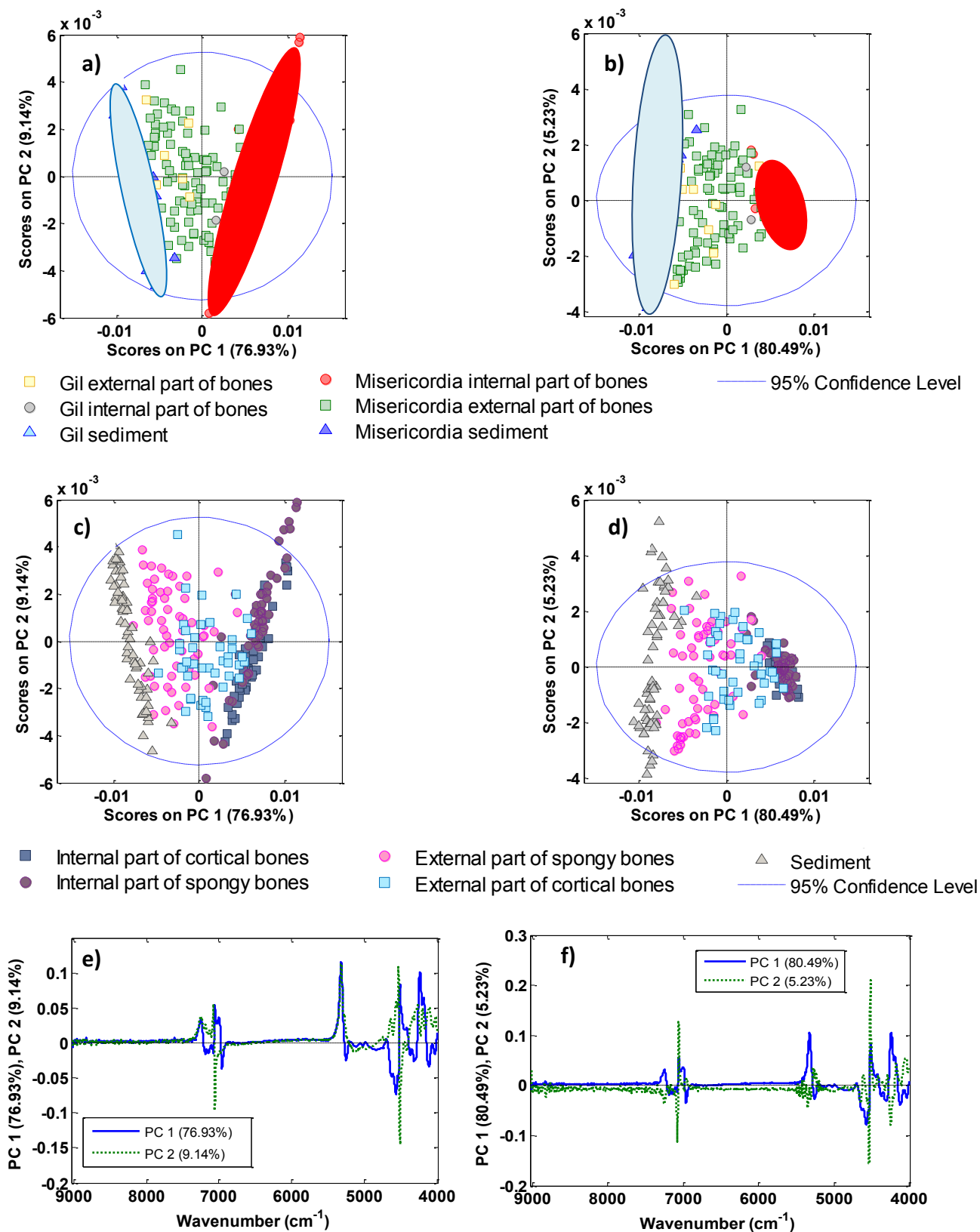
Figure 2. PLS scores and loadings graphs obtained after different spectra treatments. Score plots according Misericordia and En Gil Necropolis sample classification after: **a)** FD and MC, and **b)** MSC, FD and MC pretreatment. Score plots on considering the bone parts after: **c)** FD and MC, and **d)** MSC, FD and MC pretreatment. Loadings of PC1 and PC2 after: **e)** FD and MC, **f)** MSC, FD and MC pretreatment.
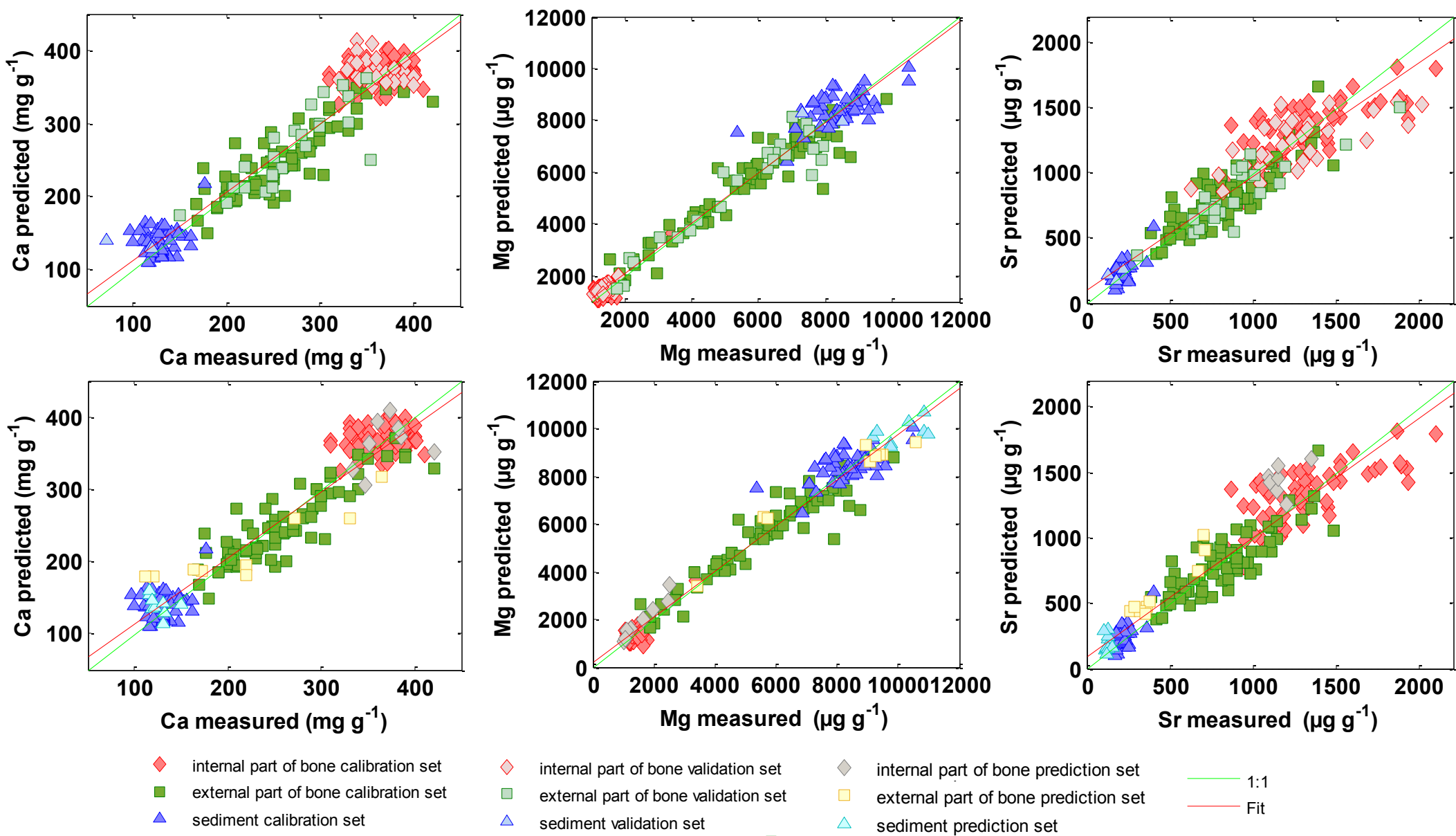
Figure 3. Regression between predicted and reference values obtained for the PLS-NIR determination of calcium, magnesium and strontium in bone remains and sediments